International Journal of Engineering & Technology, 7 (4.18) (2018) 468-472

International Journal of Engineering & Technology

Website: www.sciencepubco.com/index.php/IJET

Research paper

Effect of Grain Modification on Electrical Transport Properties and Electroresistance Behavior of $Sm_{0.55}Sr_{0.45}MnO_3$

N.Ibrahim*, Nur Azeni Mohamad Rusop, R.Rozilah, Nor Asmira, A.K.Yahya

School of Physics and Material Studies, Faculty of Applied Sciences, Universiti Teknologi MARA, 40450, Shah Alam, Selangor
**Corresponding author E-mail: noraz954@salam.uitm.edu.my*

Abstract

The structural, magnetic, electrical and electroresistance properties of $Sm_{0.55}Sr_{0.45}MnO_3$ manganites sintered at different sintering temperature of 1300°C (S1) and 1400°C (S2) had been investigated for further potential application as a nonvolatile memory elements. The samples were prepared by using conventional solid-state reaction method. An analysis of x-ray diffraction data using Rietveld analysis show that the sample crystalized in orthorhombic structure and formed pure phase. AC susceptibility measurements showed that the magnetic transition temperature remained unchanged as sintering temperature increased indicated heat treatment process does not much influence the magnetic properties of the samples. Resistivity – temperature curve with different applied currents of 1 mA and 10 mA showed metal-insulator, MI transition temperature, T_{MI} decreased with increased of the applied currents for sample S1. However, the transition temperature remained unchanged for sample S2. The increased in applied current caused the maximum resistivity around T_{MI} to be decreased for both samples indicated increased in charge carrier density which resulting in drop of resistivity, hence, enhanced double exchange mechanism. Sample S2 exhibited enhanced in ER effect in the vicinity of M-I transition temperature, T_{MI} compared to S1 sample which may relate to reduction in scattering effect as a result of reduction of grain boundary density. The observation of ER maximum behavior indicated that the materials are suitable for further investigation as a potential device for spintronic applications.

Keywords: *Conduction Mechanism; Electroresistance; Grain Modification; Manganites*

1. Introduction

The observation of electroresistance (ER), was reported in some manganites such as in $La_{0.67}Ba_{0.33}MnO_3$ [1], $Nd_{0.7}Sr_{0.3}MnO_3$ [2] and $PrMnO_3$ [3], which attributed to the changes in resistance as a results of variation of applied current/voltage [1-3]. The finding of ER effect in such manganites triggered the growth in research/study in manganites due to its potential for practical applications such as nonvolatile memory elements [1-3] and others spintronics based applications such as for communication technologies, magnetic data storage and microelectronics [4]. As reported by Mohan et al. [5], $Sm_{0.55}Sr_{0.45}MnO$ exhibited metal – insulator (MI) transition with metal-insulator transition temperature, T_{MI} of 125K under applied current of 1 mA. Interestingly, $Sm_{0.55}Sr_{0.45}MnO_3$ compound was also reported exhibited ER maximum behavior around T_{MI}. The Sm-based manganite such as $Sm_{0.55}Sr_{0.45}MnO_3$ is quite interesting compound due to presence of phase separation which was reported influence the ER effect [5, 6]. The possible mechanism for the observed ER behavior was suggested due to the improved of ordering of localized spins and the other is related to the induced of growth of ferromagnetic regions at low temperature region above T_{MI} [5]. The intensity of resistivity peak around T_{MI} of $Sm_{0.55}Sr_{0.45}MnO_3$ compound reduced when the current was increased from 2.5 mA until 50 mA. On the other hand, T_{MI} remains unchanged with increasing the electric current while insulating region near to T_{MI} drop significantly. On the other hand, another report shown that the ER effect was due to presence of inhomogeneities which related to the presence of mixed phase such as in $Sm_{0.60}Sr_{0.40}Mn_{1-x}Fe_xO_3$ compound [7]. This suggest that mechanism behind the observation of drop of resistivity as well as the existence of ER especially in Sm-based compounds could be due to other factors which need further investigation. It was also reported that the ER behavior was strongly influenced by the microstructure of the materials, such as in $Nd_{0.7}Sr_{0.3}MnO_3$ [2]. Interestingly, the modification of microstructure was also found affect the formation of inhomogeneity as well as the electrical and magnetic properties such as in $La_{0.8}Ca_{0.3}MnO_3$ compound [8]. Therefore the grain modification is also expected to have an effect on ER behavior, however, there were no details reports on how grain modification can affect the behavior of colossal ER in $Sm_{0.55}Sr_{0.45}MnO_3$. In addition to that, the microstructures of ceramic materials are strongly influenced by preparation techniques such as variation of sintering temperature [2]. Therefore, the different of sintering temperature, T_S were applied in preparation of $Sm_{0.55}Sr_{0.45}MnO_3$ compound during heat treatment process in order to investigate the effect of grain modification on ER effect behavior. The study of this $Sm_{0.55}Sr_{0.45}MnO_3$ is expected to give more explanations and knowledge about the possible mechanism involved for the observed ER behavior of the compound. Besides that, the effect of microstructure and different applied current on transport behavior was further investigated by analysis the experimental resistivity data based on scattering and hopping models both in metallic and insulating region to understand the nature of the ER behavior.

2. Methodology

$Sm_{0.55}Sr_{0.45}MnO_3$ was synthesized by the conversational solid-state synthesis method. During the preparation, stoichiometric amounts of Sm_2O_3, $SrCO_3$, and MnO_2 oxides powder with high

purity (>99.99 %) were mixed, ground and then calcined at 950 ºC for 24 hours with one intermediate grinding. After the final grinding, the powder obtained was pressed into pellet and sintered at 1300 ºC (sample S1) and 1400 ºC (sample S2), respectively for 24 hours. The structural characterization of the samples was done using X-ray diffraction (XRD) technique using a PANanalytical model Xpert PRO MPD diffractometer with CuKα radiation to determine their crystal structure and phase. The electrical and electroresistance (ER) behaviors were carried out using the standard four-point probe technique as a function of temperature (18-300 K) in a Janis model CCS 350ST cryostat under applied current of 1 mA and 10 mA, respectively. AC susceptibility measurements were carried out with variation of temperature down to 20 K and the real components were resolved using a Signal Recovery 7265 lock-in amplifier.

3. Results and Discussions

3.1. Structural Analysis

Fig. 1 shows the measured XRD diffraction pattern at room temperature with the refined diffraction pattern for $Sm_{0.55}Sr_{0.45}MnO_3$ sintered at different temperatures. The position of the diffraction peaks for both S1 and S2 samples are found similar as reported by Mohan et al. [5], Giri et al. [6] and Abramovich et al. [8]. There are no present of impurities as a result of variation in sintering temperatures. In this case, it can be said that the phase formation for the samples are not influenced by the change of sintering temperature. An analysis of diffraction data by using Rietveld refinement showed that the samples can be categorized as single-phase orthorhombic structure with lattice parameter a ≠ b ≠ c.

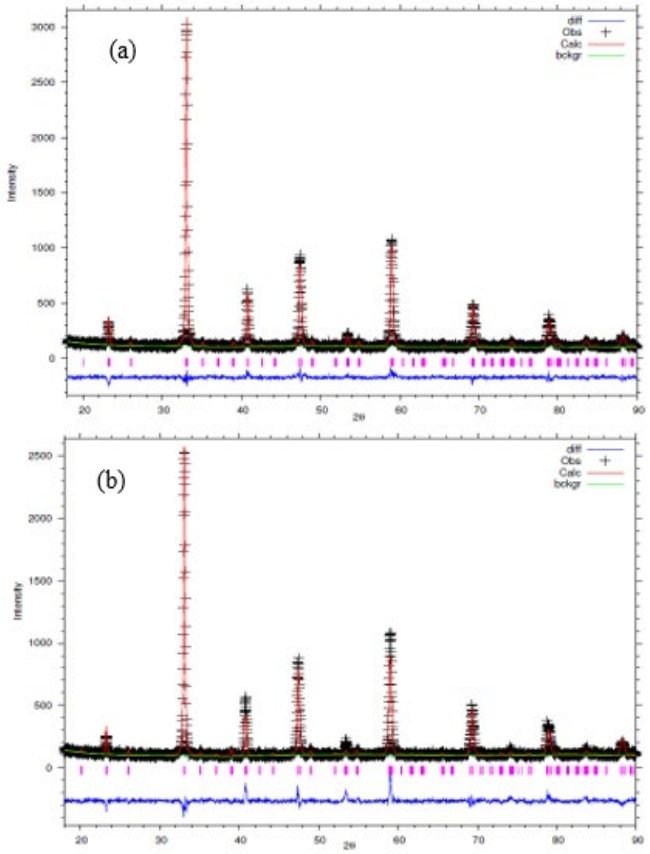

Fig. 1: Refined XRD pattern of $Sm_{0.55}Sr_{0.45}MnO_3$ (S1 and S2). The measured diffraction pattern (black curve) is shown together with the refined diffraction pattern (red curve) and their difference pattern (blue line below).

Table 1 shows the calculated lattice parameters and the unit cell volume for both samples. The obtained calculated lattice parameters for S1 (1300˚C) and S2 (1400˚C) is similar as reported in previous report by Abramovich et al. [9] and Mohan et al. [5]. It was found that unit cell volume slightly decreased as sintering temperature increased. The value of $\chi 2$ obtained is in the acceptable range which is 1.061 and 1.467 for sample S1 and S2, which reflect the high quality of fitting between experimental data and the theoretical data.

Table 1: Lattice parameters and unit cell volume of samples: $Sm_{0.55}Sr_{0.45}MnO_3$ (S1 and S2)

Sampl	a (Å)	b(Å)	c(Å)	Unit Cell Volume(Å^3)	χ^2
S1	5.4313(6)	7.6611(5)	5.4407(7)	226.39(6)	1.061
S2	5.4401(9)	7.6617(7)	5.4288(6)	226.27(7)	1.467

3.2. Magnetic Properties

Fig. 2a and 2b show the in-phase susceptibility component, χ' versus temperature for both samples S1 and S2. All samples exhibited ferromagnetic (FM) to paramagnetic (PM) transitions. For sample S1, ferromagnetic –paramagnetic transition temperature, *Tc* is observed at 134.7K as shown in the inset of Fig. 2a and 2b, while for sample S2 the Tc is at 132.2K. It is found that transition temperature slightly decreased but not much change with increased in sintering temperature, indicating the magnetic phase transition took place nearly at the same temperature. As reported by Yang et al. [10], the *Tc* of sample $La_{0.9}Te_{0.1}MnO_3$ was observed to be slightly decreased but not much change with increasing the grain size, which suggested *Tc* value not much influenced by variation of sintering temperature.

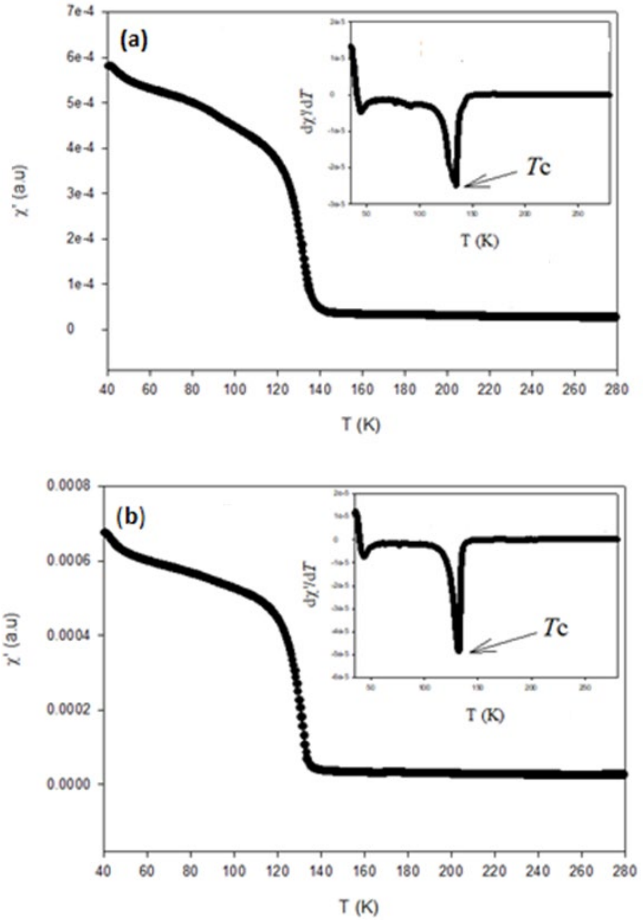

Fig. 2: Temperature dependence of real (χ') parts for both samples S1 (a) and S2 (b). Inset shows the Curie temperature, *Tc*, determined from the minima of dχ'/dT versus T curve.

The observed broad FM region indicated increased in sintering temperature influenced the growth of FM phase at low temperature region. As sintering temperature increased, the grain sizes increased as shown in Fig. 3a and 3b. For sample S1, the scanning

electron microscope (SEM) image clearly showed well formation of grain with grain size is around 2.87μm. Further, increase of sintering temperature to 1400 ˚C enlarged the grain size and improved connectivity between grains. The estimate value of grain size is around 5.96μm. The presence of large grain may cause magnetic inhomogeneity to be reduced due to reduction of grain boundaries. As suggested by Mohan et al. [5], the enlargement of grain size favors the increase of volume of FM phase due to the reduction of magnetic inhomogeneity. Hence, in this study, the increased in sintering temperature is suggested to influence the growth of FM phase which attributed to the enlargement of grain size as consequences reduction in grain boundary density.

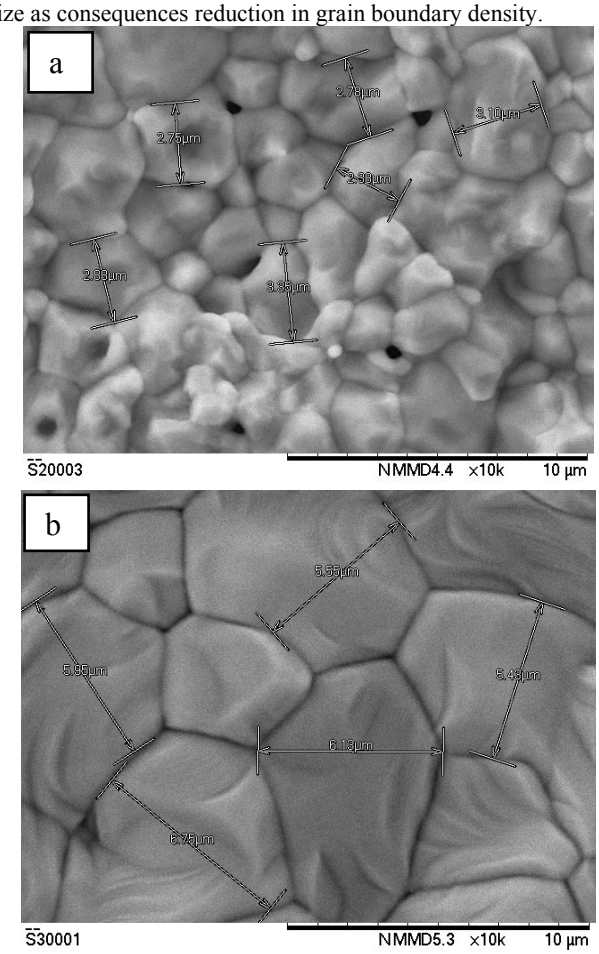

Fig. 3: Scanning Electon Micrograph with magnification of 10k for both samples, S1 (a) and S2 (b) .

3.3. Electrical Properties

Fig. 4a and 4b show the resistivity – temperature (ρ-T) curve under different applied currents of 1 mA and 10 mA, in temperature range of 20 K to 300 K for both samples S1 and S2, respectively. From the graph, the sample exhibited metallic behavior at low-temperature region below metal-insulator transition temperature, T_{MI} and above the temperature, the sample exhibited insulating behavior. The resistivity peak in the ρ vs T curve was observed at the vicinity of T_{MI}. For sample S1 which sintered at TS = 1300 ˚C, T_{MI} under applied current of 1 mA is 128.21 K, while the T_{MI} decreased to 120.58 K under applied current of 10 mA

For sample S2 which sintered at TS = 1400 ˚C, T_{MI} under same applied current of 1 mA was found to be increased to 132.18 K compared with S1 sample, while T_{MI} under applied current of 10 mA was observed remained unchanged. The similar value of T_{MI} observed under both applied current was also reported by the Mohan et al. [5] in compound $Sm_{0.55}Sr_{0.45}MnO_3$ which sintered at twice sintering processes at different temperatures. The increased in T_{MI} for sample S2 indicates microstructure modification reduced magnetic inhomogeneity due to reduction of grain boundary density as a consequence the growth of ferromagnetic phase increase and, hence double exchange (DE) mechanism enhanced. The value of resistivity peak observed at the transition temperature, T_{MI} for sample S1 under applied current of 1 mA is 422.53 Ω cm, while under applied current of 10 mA is 147.82 Ω cm. It was found that the value of resistivity at the transition temperature, T_{MI} for sample S2 under applied current of 1 mA decreased to 81.86 Ω cm compared with S1 sample, while under applied current of 10 mA, the resistivity drop to 28.45 Ω cm. Similar observation in decreasing of resistivity peak value under same applied current was also reported by the Mohan et al. [5] in compound $Sm_{0.55}Sr_{0.45}MnO_3$. For both samples, the increased in applied current caused resistivity to drop, hence, conductivity increased which indicated that the number of charge carrier increased. The increased in charge carrier concentration is suggested due to applied electric field improved spin alignment of e_g of charge carrier, hence, DE mechanism enhanced. Under applied electric field, free charge carriers may have enough energy to overcome the insulating barrier at grain boundary region as consequences interfacial polarization process increased and, hence, decreased in resistivity as well as induced electroresistance (ER) effect as it is described in Fig. 5.

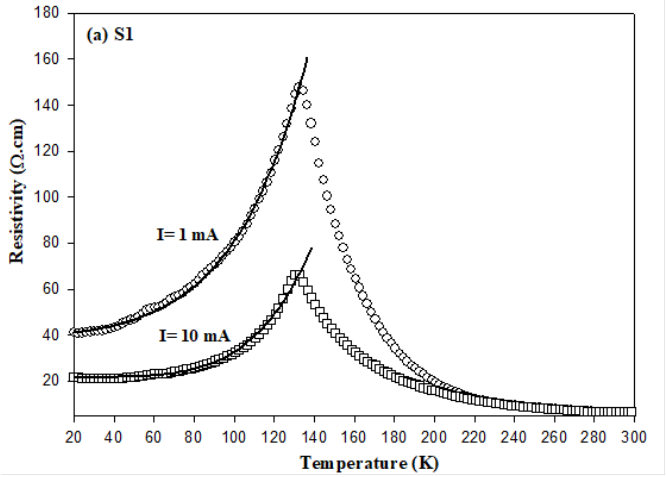

Fig. 4a: Resistivity–temperature plot of sample S1 (TS = 1300˚C) under applied current of 1 mA and 10 mA, respectively. The solid lines show the fitting made to the equation $\rho = \rho 0 + \rho_2 T^2 + \rho_5 T^5$

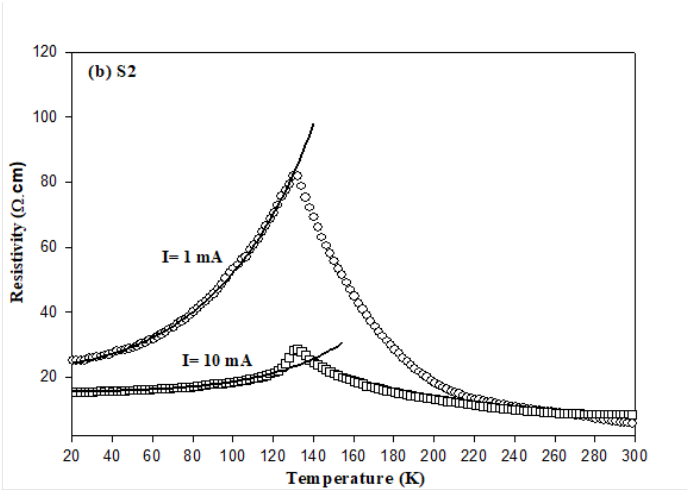

Fig. 4b: Resistivity–temperature plot of sample S2 (TS = 1400˚C) under applied current of 1 mA and 10 mA, respectively. The solid lines show the fitting made to the equation $\rho = \rho 0 + \rho_2 T^2 + \rho_5 T^5$

Fig. 5 describes the temperature dependence of electroresistance (ER %) for both samples S1 and S2. The ER, is defined as $[\rho(I_1) - \rho(I_2)] / \rho(I_2)] \times 100\%$ [5] where $\rho(I_1)$and $\rho(I_2)$ are the resistivi-

ties of the sample at applied current of I_1 = 1mA and I_2= 10 mA, respectively. As shown in Fig. 5, for sample S2, ER maximum about 230 % is observed at the vicinity of T_{MI} while for sample S1, ER maximum is 140 % observed slightly below T_{MI}. The differences in ER maximum values for both samples, S1 and S2 may relate to the microstructure modification. Sample S1 which has smaller grain size compared to sample S2 showed smaller ER effect around T_{MI} compared to S2 sample. The findings showed that the increased in grain size enhanced the ER effect around T_{MI} which may relate to the formation of homogeneous grain as well as reduction in grain boundary density compared to sample S1, which influenced the resistance behavior. For sample S1, large grain boundary density may result to the increased in formation of magnetic inhomogeneity which was not much affected by the increased of applied current results in smaller change of resistivity at the vicinity of T_{MI} compared to sample S2 and as a consequence of smaller ER effect is observed for sample S1. For sample S2, it is suggested that the ordering of localized spins increased under increased of applied current and, hence, spin scattering of charge carrier reduced [9] which contribute to the large change of resistivity at the vicinity of T_{MI} and the observed large ER effect. The reduction of resistivity above T_{MI} in insulating region for both samples indicated increased in applied current enhanced the polarization of charge carrier at the grain boundaries region which may relate to the growth of FM phase and reduction of phase separated. The connectivity between FM cluster may form the percolative path for the currents to flow in insulating region and, hence, result in reduction of resistivity and the observation of ER effect [11].

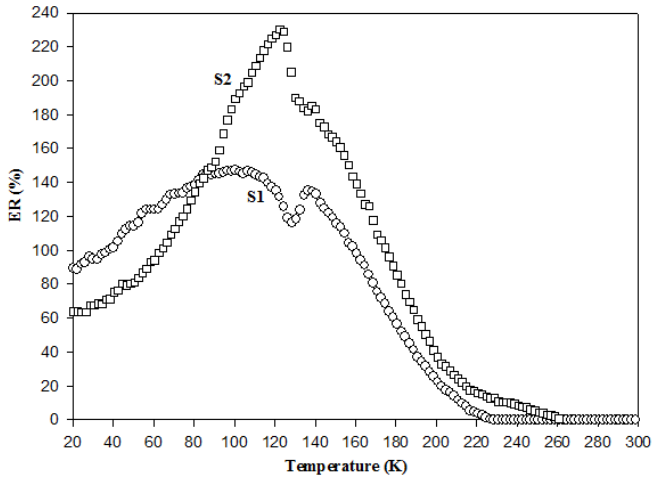

Fig. 5: Temperature dependence of electroresistance , ER for S1 and S2 samples.

The observed ER behaviour can be further understood by fitting the experimental resistivity data to the scattering models [12-14] in order to elucidate the possible mechanism involve for the-observed behavior. In the FM region below T_{MI}, the resistivity can be explained by the $\rho = \rho_0 + \rho_2 T^2 + \rho_5 T^5$. The first term of ρ_0 represents the contribution of resistivity due to grain effect, while the second term of $\rho_2 T^2$ represents the electron-electron scattering contribution to the resistivity and $\rho_5 T^5$ represents the contribution to the resistivity due to electron-phonon scattering [13, 14]. As shown in Table 2, for both samples, the increased in applied current reduced the scattering effect as all the values of scattering parameter ρ_0, ρ_2 and ρ_5 decreased with increased of applied current. The increased in applied current is found decreased in scattering effect caused the resistivity to decrease and, hence, induce the ER effect. In addition, the value of all parameters are smaller for sample S2 when compared with sample S1 suggested that scattering effect reduced as a result of grain modification. To understand the charge transport in insulating region above T_{MI}, the resistivity data was fitted using variable range hopping VRH model which represented by the empirical equation of $\rho = \rho_0 \exp(T_0/T)^{1/4}$ [12-14]. Fig. 6a and 6b show the linear fitting of ln ρ vs $T^{-1/4}$ plots for both samples. As can be seen from Table 3, the hopping energy, E_h reduced with increased applied current which may relate to increase of delocalization of charge carrier due to less scattering effect and, hence, less energy is required for the hopping process. E_h is calculated based on the relation of $E_h(T) = 1/4 k_B (T)^{3/4} (T_{om})^{1/4}$ where T_{om} is the Mott characteristic temperature and is related to carrier localization length which can be obtained from the slope of the graph of ln ρ vs $T^{-1/4}$ and k_B is Boltzman's constant. Further, E_h was found to be significantly reduced for sample S2 which suggested enlarged in grain size further reduced the scattering effect and, hence, number of delocalization of charge carrier increased as shown by the increase of value of density of state at fermi level, $N(E_F)$ in Table 3. $N(E_F)$ was calculated using the equation of $N(E_F) = 18/ k_B T_{om}$, where α is the localization length and the value of α has been taken as 4.5 Å for the calculation to estimate the value of $N(E_F)$ [13, 14].

Table 2: Best fitted parameters obtained from fitting experimental data in the metallic region to equations $\rho = \rho_0 + \rho_2 T^2 + \rho_5 T^5$ of 1 mA and 10 mA for S1 and S2 samples.

Sample	ρ_0(x10^1) (Ω.cm)		ρ_2(x10^{-3})(Ω.cmK^{-2})		ρ_5(x10^{-9})(Ω.cm K^{-5})	
	I = 1 mA	I = 10 mA	I = 1 mA	I = 10 mA	I = 1 mA	I = 10 mA
S1	4.0083	2.1601	2.5000	0.2947	1.5548	1.0876
S2	2.3352	1.5354	2.3000	0.2000	0.5246	0.1140

Table 3: Best fitted parameters obtained from VRH model fitting under magnetic fields of 1 mA and 10 mA for S1 and S2 samples. The E_h and R_h values are calculated at T = 200K

Sample	T_o(x10^7 K)		E_h (200 K) (meV)		R_h(200 K) (x10^{-7})		$N(E_F)$/(x10^{20}) (eV^{-1}cm^{-3})	
	I = 1 mA	I = 10 mA	I = 1 mA	I = 10 mA	I = 1 mA	I = 10 mA	I = 1 mA	I = 10 mA
S1	3.07	0.43	85.27	52.23	3.34	2.05	0.75	5.30
S2	0.60	0.03	56.71	25.63	2.22	1.00	3.81	91.38

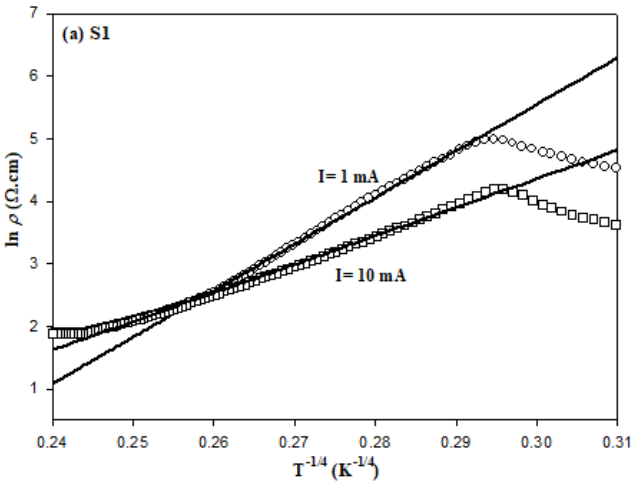

Fig. 6a: Resistivity–temperature plot of sample S1 (TS = 1300˚C) under applied current of 1 mA and 10 mA, respectively. The solid lines show the best fitting made to the small variable range hopping, VRH model.

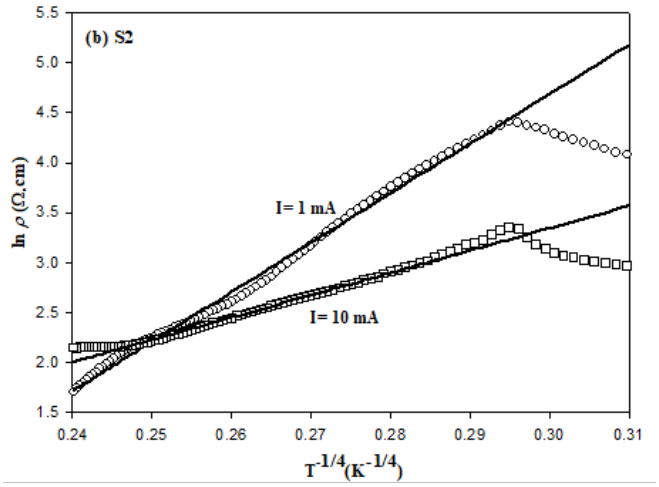

Fig. 6b: Resistivity–temperature plot of sample S2 (TS = 1400˚C) under applied current of 1 mA and 10 mA, respectively. The solid lines show the best fitting made to the small variable range hopping, VRH model.

4. Conclusion

The samples of $Sm_{0.55}Sr_{0.45}MnO_3$ were prepared using solid state method which were sintered at different temperatures, which is at 1300 ^oC (S1) and 1400 ^oC (S2), respectively. It has been found that grain modification influenced the ER effect. Sample S2 with enlarged of grain size showed increased in ER maximum effect due to reduction of magnetic inhomogeneity in presence of increase of applied current. The effect of grain modification on the magnetic properties of sample has been studied by measuring AC magnetic susceptibility at temperature range from 40 K to 280 K. It has been found that grain modification does not much influence the magnetic properties as *Tc* remains almost constant for both samples, S1 and S2. The observed of enhanced ER effect at the vicinity of T_{MI} may relate to the combination of reduction of scattering effect together with the improved in connectivity between ferromagnetic phase as a result of the enlargement of grain size for sample S2.

Acknowledgement

We would like to express gratitude to Malaysian Ministry of Higher Education (MOHE) and Institute of Research Management and Innovation (IRMI), Universiti Teknologi MARA through the Fundamental Research Grant Scheme (FRGS) [Ref: 600-RMI/FRGS 5/3 (76/2016).

References

[1] Kumar R, Gupta AK, Kumar V, Bhalla GL and Khare N (2007), Temperature dependence of electroresistance for $La_{0.6}Ba_{0.33}MnO_3$ manganite, *Journal of Physics and Chemistry of Solids* 68, 2394-2397.

[2] Chen SS, Yang CP and Dai Q (2010), Effect of microstructure on the electroresistance of $Nd_{0.7}Sr_{0.3}MnO_3$ perovskite ceramics, *Journal of Alloys and Compounds* 491, 1-3.

[3] Keshvani MJ et al (2017), Studies on structural, morphology and electroreristance properties of sol-gel method nanostructured $PrMnO_3$, *Materials Science and Engineering B* 218, 40-50.

[4] Solanki PS, Khachar U, Vagadia M, Ravalia A, Katba S and Kuberkar DG (2015). Electroresistance and field effect studies on manganite based heterostructure, *Journal of Applied Physics* 117, 145306.

[5] Mohan R, Kumar N, Singh B, Gaur NK, Bhattacharya S, Rayaprol S, Dogra A., Gupta SK, Kim SJ and Singh RK (2010), Colossal electroresistance in $Sm_{0.55}Sr_{0.45}MnO_3$, *Journal of Alloys and Compounds* 508, L32-L35.

[6] Giri S, Dasgupta K, Poddar A, Nigam AK and Nath TK (2014), Field induced ferromagnetic phase transition and large magnetocaloric effect in $Sm_{0.55}Sr_{0.45}MnO_3$ phase separated manganites, *Journal of Alloys and Compounds* 582, 609-616.

[7] Mahmud ST, Saber MM, Alagoz H S, Biggart K, Bouveyron R, Mahmud Khan, Jung J and Chow KH (2012), Disorder enhanced intrinsic electroresistance in $Sm_{0.60}Sr_{0.40}Mn_{1-x}Fe_xO_3$, Appl. Phys. Lett., 100, 2320406

[8] Siwach PK, Prasad R, Gaur A, Singh HK, Varma GD and Srivastava ON (2007), Microstucture-magnetotransport correlation in La0.7Ca0.3MnO3, *Journal of Alloys and Compounds* 443, 26-31.

[9] Abramovich AI, Koroleva LI., Michurin AV, Gorbenko OY and Kaul AR (2000), Relationship between colossal magnetoresistance and giant magnetostriction at Curie point in $Sm_{0.55}Sr_{0.45}MnO_3$, *Physica B*: *Condensed Matter* 293, 38-43.

[10] Yang J et al (2004), The effect of grain size on electrical and magnetic properties of $La_{0.9}Te_{0.1}MnO_3$, *Solid State Communications* 132, 83-87.

[11] Li Zhang, Xia Li, Feifei Wang, Tao Wang and Wangzhou Shi (2013), Colossal electroresistance and magnetoresistance effect in polycrystalline perovskite cobaltites $Nd_{1-x}Sr_xCoO_3$ (x= 0.1, 0.2, 0.3), *Materials Research Bulletin* 48, 1088-1092.

[12] Nagaraja BS, Ashok Rao, Poornesh P, Tarachand and Okram, GS (2017), Investigation on structural, electrical, magnetic and thermoelectric properties of low bandwidth Sm1-xSrxMnO3 (0.2<x< 0.5) manganites, *Physica B*: *Condensed Matter* 523, 67-77.

[13] Rozilah R, Ibrahim N, Mohamed Z, Yahya AK, Nawazish A. Khan, M. Nasir Khan, (2017), Inducement of ferromagnetic-metallic phase in intermediate-doped charge-ordered $Pr_{0.75}Na_{0.25}MnO_3$ manganite by K+ substitution, *Physica B*: *Condensed Matter* 521 , 281–294.

[14] Nor Asmira, Ibrahim N, Mohamed Z, Yahya AK (2018), Effect of Cr^{3+} substitution at Mn-site on electrical and magnetic properties of charge ordered $Bi_{0.3}Pr_{0.3}Ca_{0.4}MnO_3$ manganites, *Physica B*: *Condensed Matter* 544, 34–46.